

Exploring the effect of aggregation-induced emission on the excited state intramolecular proton transfer for a bis-imine derivative by quantum mechanics and our own *n*-layered integrated molecular orbital and molecular mechanics calculations

Huifang Zhao(赵慧芳), Chaofan Sun(孙朝范), Xiaochun Liu(刘晓春), Hang Yin(尹航), Ying Shi(石英)

Citation: Chin. Phys. B . 2019, 28(1): 018201. **doi:** 10.1088/1674-1056/28/1/018201
Journal homepage: http://cpb.iphy.ac.cn; http://iopscience.iop.org/cpb

What follows is a list of articles you may be interested in

Effect of intramolecular and intermolecular hydrogen bonding on the ESIPT process in DEAHB molecule

Hui Li(李慧), Lina Ma(马丽娜), Hang Yin(尹航), Ying Shi(石英)

Chin. Phys. B . 2018, 27(9): 098201. **doi:** 10.1088/1674-1056/27/9/098201

Theoretical investigation on the excited state intramolecular proton transfer in Me_2N substituted flavonoid by the time-dependent density functional theory method

Hang Yin(尹航), Ying Shi(石英)

Chin. Phys. B . 2018, 27(5): 058201. **doi:** 10.1088/1674-1056/27/5/058201

Ultrafast structural dynamics studied by kilohertz time-resolved x-ray diffraction

Guo Xin, Jiang Zhou-Ya, Chen Long, Chen Li-Ming, Xin Jian-Guo, Peter M. Rentzepis, Chen Jie

Chin. Phys. B . 2015, 24(10): 108701. **doi:** 10.1088/1674-1056/24/10/108701

Exploring the effect of aggregation-induced emission on the excited state intramolecular proton transfer for a bis-imine derivative by quantum mechanics and our own *n*-layered integrated molecular orbital and molecular mechanics calculations*

Huifang Zhao(赵慧芳), Chaofan Sun(孙朝范), Xiaochun Liu(刘晓春), Hang Yin(尹航)†, and Ying Shi(石英)‡

Institute of Atomic and Molecular Physics, Jilin University, Changchun 130012, *China*

(Received 19 October 2018; revised manuscript received 9 November 2018; published online 21 December 2018)

We theoretically investigate the excited state intramolecular proton transfer (ESIPT) behavior of the novel fluorophore bis-imine derivative molecule HNP which was designed based on the intersection of 1-(hydrazonomethyl)-naphthalene-2-ol and 1-pyrenecarboxaldehyde. Especially, the density functional theory (DFT) and time-dependent density functional theory (TDDFT) methods for HNP monomer are introduced. Moreover, the "our own *n*-layered integrated molecular orbital and molecular mechanics" (ONIOM) method (TDDFT:universal force field (UFF)) is used to reveal the aggregation-induced emission (AIE) effect on the ESIPT process for HNP in crystal. Our results confirm that the ESIPT process happens upon the photoexcitation for the HNP monomer and HNP in crystal, which is distinctly monitored by the optimized geometric structures and the potential energy curves. In addition, the results of potential energy curves reveal that the ESIPT process in HNP will be promoted by the AIE effect. Furthermore, the highest occupied molecular orbital (HOMO) and lowest unoccupied molecular orbital (LUMO) for the HNP monomer and HNP in crystal have been calculated. The calculation demonstrates that the electron density decrease of proton donor caused by excitation promotes the ESIPT process. In addition, we find that the variation of atomic dipole moment corrected Hirshfeld population (ADCH) charge for proton acceptor induced by the AIE effect facilitates the ESIPT process. The results will be expected to deepen the understanding of ESIPT dynamics for luminophore under the AIE effect and provide insight into future design of high-efficient AIE compounds.

Keywords: time-dependent density functional theory (TDDFT) method, excited state intramolecular proton transfer (ESIPT), our own *n*-layered integrated molecular orbital and molecular mechanics (ONIOM) method, potential energy curves, atomic dipole moment corrected Hirshfeld population (ADCH) charge

PACS: 82.39.Jn, 31.15.ee, 87.15.ht **DOI:** 10.1088/1674-1056/28/1/018201

1. Introduction

Molecules that exhibit the excited state intramolecular proton transfer (ESIPT) property, first explored by Weller,[1] have attracted considerable attention since they have important applications for green fluorescent protein,[2] for use in bioimaging,[3] as organic light emitting diodes,[4] as fluorescent chemosensors,[5–7] and in photophysical studies.[8–19] It is well known that the molecules exhibiting the ESIPT properties involve a heterocyclic ring which is formed by the intramolecular hydrogen bond between a hydroxyl group and a neighboring proton acceptor. Most of the reported organic chromophores with ESIPT property are highly emissive in solution with high fluorescence quantum efficiencies, but weakly emissive (or non-fluorescent) in a rigid medium due to the aggregation-caused quenching mechanism.[19–22] To achieve solid state emission, it is necessary to suppress other radiationless deactivation pathways which occur at the excited state by aggregation-induced emission (AIE) effect.[23] Recently, the development of AIE–ESIPT dual mechanism based fluorophores has attracted extensive interest. Dwivedi *et al.* have discovered that the ESIPT emission for derivatives of 2-hydroxy-3-(quinazolin-2-yl)-benzaldehyde (HQz1–HQz6) gets completely quenched in solvents with diverse polarities which have been restored by AIE.[24] In addition, Samanta *et al.* designed and synthesized a novel fluorophore bis-imine derivative molecule HNP which was based on the intersection of 1-(hydrazonomethyl)-naphthalene-2-ol and 1-pyrenecarboxaldehyde.[25] It also had the potential to tune several emission colors with variations of the water fraction in a methanol–water mixture, owing to the AIE and ESIPT phenomena. Especially, the AIE effect could regulate the ratio of dual fluorescence and enhance the emission from ESIPT state.[25] The 1-(hydrazonomethyl)-naphthalene-2-ol[26] part has exclusively intramolecular O–H···N hydrogen bonds, which forms a rather strong quasi-aromatic chelating ring, possessing a potential possibility for proton transfer. Moreover, as pyrene more often participates in self-assembly to

*Project supported by the National Natural Science Foundation of China (Grant Nos. 11574115 and 11704146).

†Corresponding author. E-mail: yinhang@jlu.edu.cn

‡Corresponding author. E-mail: shi_ying@jlu.edu.cn

© 2019 Chinese Physical Society and IOP Publishing Ltd

generate excimer emissions, the introduction of a pyrene moiety might provide an AIE property.[27,28] However, the detailed mechanism of the AIE effect facilitating the ESIPT process, which enhances the emission from ESIPT state, is not completely clear so far for the molecule. Therefore, it is necessary to clarify the AIE behavior in the light of ESIPT processes in depth by theoretical research.

In the present work, the HNP molecule is theoretically investigated to provide the details of AIE effect on the ESIPT process. We have carried out the time-dependent density functional theory (TDDFT) calculations to systematically explore the ESIPT phenomenon, as well as the quantum mechanics:molecular mechanics (QM:MM) calculations with our own *n*-layered integrated molecular orbital and molecular mechanics (ONIOM) scheme[29–31] to reveal the AIE mechanism. The results will be expected to deepen the understanding of photophysics for luminophore with the AIE–ESIPT property and provide insight into the future design of high-efficient AIE compounds.

2. Computation methods

In the present work, the density functional theory (DFT) and TDDFT[32–40] methods are introduced to perform the ground-state and electronic excited-state geometry optimizations, respectively. The Becke's three-parameter hybrid exchange function with Lee-Yang-Parr gradient-corrected correlation (B3-LYP)[41,42] functional and the triple-ζ valence quality with one set of polarization functions (TZVP) basis set[43] are used in our DFT and TDDFT calculation throughout. Moreover, no constrains for symmetry, bonds, angles, or dihedral angles are employed in the geometry optimization calculations. In addition, a similar strategy at the ONIOM[29–31] (TDDFT:universal force field (UFF)) level is used for the AIE mechanisms calculation. The initial structures of ONIOM calculations are set up by subtracting a 45-molecule cluster (2205 atoms in total) from crystal structure reported by Samanta *et al.*,[25] in which one HNP luminophore in the middle was set as model part and treated by high-level QM calculations, while the surrounding molecules were computed by low-level UFF force field[44] with charge equilibration (QEQ)[45] charges. During geometry optimization, only the QM molecule is allowed to move.[46] This electron-localized model is not able to describe the physical picture of the excited crystal precisely, but it can be supposed to be sufficient for the purpose of the study. In ONIOM calculations, an electronic embedding (ONIOM-EE)[47] scheme is employed, which incorporates the electrostatic interaction in the QM Hamiltonian and allows the wave function to be polarized by the charge distribution of MM region. All the electronic structure calculations are carried out using the Gaussian 09 program suite.[48] Moreover, further processing of data is executed using the Multiwfn 3.5 program suite.[49]

The nomenclatures are explained as follow: the results without particular illustration are calculated for HNP monomer with QM method, while those starting with "c" are obtained in crystal by ONIOM (QM:MM) method.

3. Results and discussion

3.1. Optimized geometric structures

The geometric conformations of the enol (S_0), enol* (S_1), and keto* (S_1) forms have been optimized and shown in Fig. 1 to depict the ESIPT mechanism for HNP monomer. We can obtain that two intramolecular hydrogen bonds (IMHBs) are formed from the optimized geometries: one is formed between N_1 and H_2 in the enol and enol* form, while the other is formed between O_1 and H_2 in the keto* form. Furthermore, the numerical values of the key geometric parameters of different electronic states can be obtained from Table 1. Obviously, being excited to enol* state, the distance between N_1 and H_2 decreases from 1.691 Å to 1.643 Å; meanwhile, the bond length between O_1 and H_2 increases from 0.999 Å to 1.012 Å. In addition, the bond angle $O_1C_{15}C_3$ in enol* state is smaller than that in enol form and there exists a relatively small change in enol* state bond angles $C_{18}C_3C_{15}$ comparing with the corresponding ground state bond angles. It signifies that after being excited, the hydrogen bonded quasi-aromatic chelating ring becomes smaller. And the interactions between the involved atoms should increase as the spacing between atoms decreases. Clearly, the IMHB becomes shorter so that the interaction between N_1 and H_2 increases, which implies that the H_2 has the tendency to depart from the proton donor

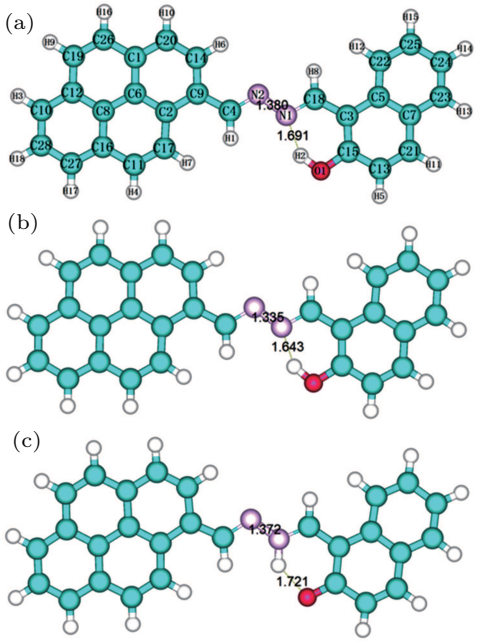


Fig. 1. Schematic plots of the HNP structure optimized at the S_0 and S_1 states in the (a) enol, (b) enol*, and (c) keto* forms.

O_1 and get close to the proton acceptor N_1. Subsequently, the HNP evolves into the keto* form, i.e., the H_2 transfers from O_1 to N_1. Specifically, the IMHB between N_1 and H_2 turns into a covalent bond, concomitantly the new IMHB between O_1 and H_2 is formed. Therefore, the intramolecular hydrogen bond in the HNP monomer facilitates the ESIPT process.

To reveal the AIE effect on the geometric conformations, we provide the optimized c-enol (S_0), c-enol* (S_1), and c-keto* (S_1) forms for HNP in crystal, as shown in Fig. 2. And the numerical values of the key geometric parameters of different electronic states are shown in Table 1. It is worth noting that, under the AIE effect, there is a distinct difference between enol* and c-enol* state. Especially, the N_1–N_2 is shorter in c-enol* state than that in enol* state, which means that the interaction between N_1 and N_2 is enhanced by the AIE effect. More detailed information about the variation of N_1–N_2 bond is investigated in the discussion below.

Table 1. Calculated bond lengths (Å), bond angles (degree) of HNP and c-HNP in different electronic states.

	N_1–N_2	N_1–H_2	O_1–H_2	O_1–C_{15}	C_3–C_{15}	C_3–C_{18}	N_1–C_{18}	N_1–O_1	$C_{18}C_3C_{15}$	$O_1C_{15}C_3$
Enol	1.380	1.691	0.999	1.337	1.407	1.440	1.297	2.584	119.986	122.717
Enol*	1.335	1.643	1.012	1.330	1.433	1.428	1.321	2.559	120.407	121.662
Keto*	1.372	1.045	1.721	1.260	1.458	1.445	1.298	2.582	118.922	121.697
c-Enol	1.377	1.661	1.006	1.342	1.404	1.443	1.294	2.570	120.068	122.202
c-Enol*	1.244	1.810	0.974	1.370	1.406	1.429	1.322	2.672	122.602	122.046
c-Keto*	1.376	1.050	1.651	1.266	1.451	1.448	1.295	2.545	118.679	121.648

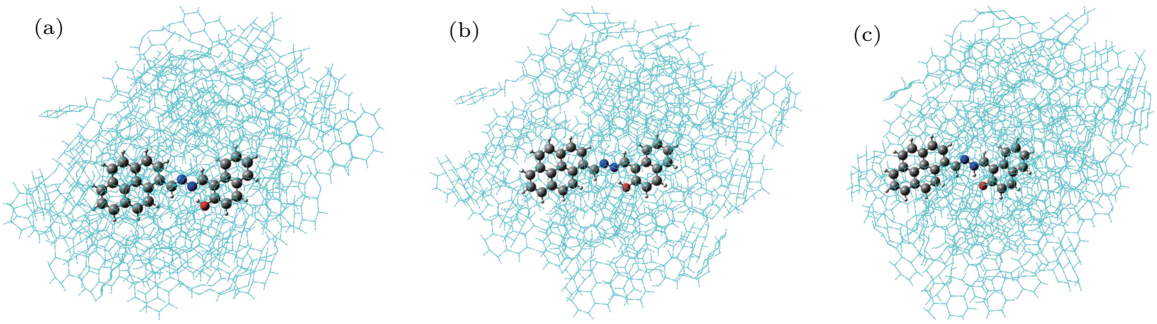


Fig. 2. Schematic plots of the c-HNP structure optimized at the S_0 and S_1 states in the (a) enol, (b) enol*, and (c) keto* forms.

3.2. Frontier molecular orbitals

To investigate the nature of the excited state for the HNP, the analyses of the frontier molecular orbits for HNP monomer and HNP in crystal are introduced. Through the TDDFT calculation, we demonstrate that the S_1 states of the HNP monomer and HNP in crystal correspond to the HOMO→LUMO transition. The frontier molecular orbital (HOMO and LUMO, c-HOMO and c-LUMO) are shown schematically in Fig. 3. And we can discover that the HOMOs and LUMOs exhibit the π and π^* character, respectively. That is to say, the S_1 states have the $\pi\pi^*$ feature which is believed to facilitate the proton transfer.[34,42] Clearly, the electron density on O_1 in the LUMO decreases in comparison with that in HOMO for both HNP monomer and HNP in crystal. Interestingly, the electron density of O_1 atom which is directly involved in the ESIPT process, as mentioned above, decreases a lot after being excited to the S_1 state. Furthermore, the electrostatic attraction between O_1 and H_2 decreases due to the reduced electron density around O_1 after being excite. Therefore, we suggest that the electron density change of O_1 due to the intramolecular charge redistribution upon excitation is not only tightly associated with changes of the acid–base properties of hydroxyl group and carbonyl group, but also promotes the ESIPT due to the reduction in proton control.

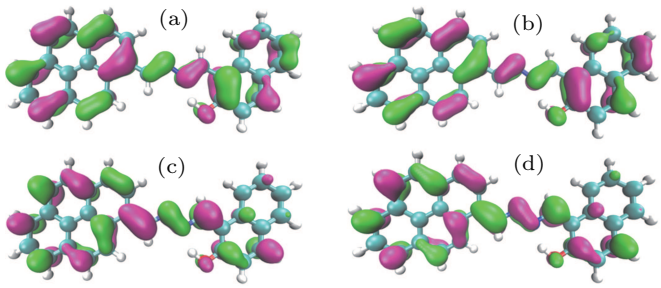


Fig. 3. Schematic plots of frontier molecular orbitals: (a) HOMO and (b) LUMO for HNP, and (c) HOMO and (d) LUMO for c-HNP.

3.3. Potential energy curves

In order to demonstrate the details of the ESIPT process and explore the mechanism for de-excitation for HNP upon excitation to the S_1 state, the calculations of the potential energy curves of HNP monomer and HNP in crystal at different electronic states are introduced. The potential energy curves of the ground state and the excited state for the HNP molecule

are optimized by fixing the spacing between O_1 and H_2 (proton transfer coordinate) at different values, which are recorded in Fig. 4 for HNP monomer and in Fig. 5 for c-HNP. Form Fig. 4, two stable geometries in S_1 state which are respectively corresponding to the enol* form and keto* form can be discovered. It depicts that there are two stable equilibrium geometries for HNP monomer after Frank–Condon transition to the S_1 state. The H_2 will transfer from O_1 to N_1 to achieve the equilibrium geometry of S_1 state tautomer form. Consequently, a new hydrogen bond between N_1 and H_2 can be formed. Indeed, the existence of S_1 state tautomer equilibrium geometry can act as the direct evidence for the ESIPT process for HNP monomer. In addition, a similar phenomenon also exists in c-HNP. On the other hand, it is noteworthy that the transferred H_2 needs to move about 0.2 Å to cross the barrier in S_1 state for HNP monomer, whereas only 0.1 Å for HNP in crystal through comparing Fig. 4 with Fig. 5. That is to say, under the AIE effect, the moving distance of transferred proton to overwhelm the barrier decreases. Moreover, the energy of keto* state is 0.04 eV lower than the enol* state for HNP and it is 0.15 eV for c-HNP, which means that the keto* state fluorescence will be promoted by the AIE effect. It is because that the lower energy for keto* state leads to Keto* state fluorescence enhancement.[50]

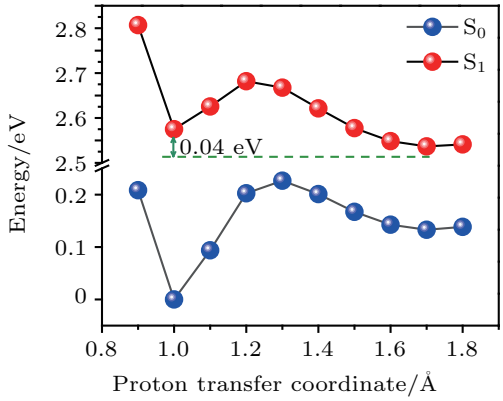


Fig. 4. Calculated potential energy curves along the proton transfer coordinate (O_1–H_2) of HNP in different electronic states.

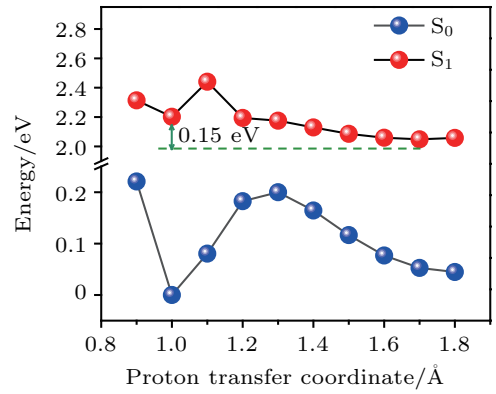


Fig. 5. Calculated potential energy curves along the proton transfer coordinate (O_1–H_2) of c-HNP in different electronic states.

3.4. Atomic charge distribution

To further investigate the mechanism of AIE effect on the ESIPT process, we calculate the atomic dipole moment corrected Hirshfeld population (ADCH) charge and Mayer bond order of enol* state and c-enol* state, which are the reactants in the ESIPT phenomenon, for HNP monomer and HNP in crystal, respectively. In addition, the numerical values of the key parameters can be found in Table 2. As mentioned in the section of optimized geometric structures, there is an interesting decrease of the bond length of N_1–N_2 in c-enol* state comparing with that in enol* state. Moreover, from Table 2, we can see that the Mayer bond order for N_1–N_2 of c-enol* state is larger than that in enol* state. There is a consistence between the above two results which are obtained. It means that the AIE effect enhances the interaction between N_1 and N_2 in enol* state. From Table 2, the ADCH charge of N_1 which is the proton acceptor directly involved in the ESIPT process can also be obtained. It is worth nothing that the AIE effect makes the ADCH charge of N_1 from positive value to negative value, which increases the attraction to the transferred proton. Meanwhile, the AIE effect also makes the ADCH charge of N_2 from -0.252 to -0.081. Therefore, we demonstrate that the bond length change of N_1–N_2 and the variation of ADCH charge for N_1 and N_2 in c-enol* state by the AIE effect, which causes the enhancement of interaction between proton acceptor and transferred proton, facilitate the ESIPT process.

Table 2. ADCH charge and Mayer bond order of enol* state for HNP monomer and c-enol* state for HNP in crystal.

	N_1	N_2	H_2	N_1–N_2
Enol*	0.002	−0.252	0.170	1.110
c-Enol*	−0.054	−0.081	0.317	1.414

4. Conclusions

The QM (TDDFT) method has been used to investigate the details of the ESIPT process for the HNP monomer, and the ONIOM (TDDFT:UFF) method has been introduced for HNP in crystal to perform the AIE effect on the ESIPT process. For the HNP monomer, the calculation of geometric structures reveals that the interaction between N_1 and H_2 increases upon excitation due to the shorter IMHB, and subsequently the H_2 transfers from O_1 to N_1. Through the calculation of HOMO and LUMO, we demonstrate that the electron density decrease of O_1 due to the intramolecular charge redistribution in the S_1 state promotes the ESIPT. In addition, the results of calculated potential energy curves act as a direct evidence for the ESIPT (enol*→ keto*) and explain the dual fluorescence spectral feature. As for the HNP in crystal, the calculation of geometric structures indicates that N_1–N_2 is shorter in c-enol* state than that in enol* state. In addition, the results of calculated potential energy curves show that the moving distance of the transferred proton to overwhelm the barrier decreases under

the AIE effect. Moreover, through the calculation of ADCH charge and Mayer bond order in enol* state and c-enol* state, we find that the variation of ADCH charge for N_1 and N_2 in c-enol* state due to the AIE effect facilitates the ESIPT process. These results are helpful for us to deepen the understanding of photophysics for luminophore under AIE effect and contribute to the further design of high-efficient AIE compounds.

Acknowledgment

We express heartfelt thanks to other members of our discussion group for their valuable comments.

References

[1] Weller A 1956 *Ber. Bunsenges. Phys. Chem.* **60** 1144
[2] Zheng D Y, Zhang M Z and Zhao G J 2017 *Sci. Rep.* **7** 13766
[3] Shynkar V V, Klymchenko A S, Kunzelmann C, Duportail G, Muller C D, Demchenko A P, Freyssinet J M and Mely Y 2007 *J. Am. Chem. Soc.* **129** 2187
[4] Tang K C, Chang M J, Lin T Y, Pan H A, Fang T C, Chen K Y, Hung W Y, Hsu Y H and Chou P T 2011 *J. Am. Chem. Soc.* **133** 17738
[5] Zhao J Z, Ji S M, Chen Y H, Guo H M and Yang P 2012 *Phys. Chem. Chem. Phys.* **14** 8803
[6] Shiraishi Y, Matsunaga Y, Hongpitakpong P and Hirai T 2013 *Chem. Commun.* **49** 3434
[7] Liu B, Wang H, Wang T S, Bao Y Y, Du F F, Tian J, Li Q B A and Bai R K 2012 *Chem. Commun.* **48** 2867
[8] Demchenko A P, Tang K C and Chou P T 2013 *Chem. Soc. Rev.* **42** 1379
[9] Klymchenko A S 2017 *Acc. Chem. Res.* **50** 366
[10] Cheng X, Wang K, Huang S, Zhang H Y, Zhang H Y and Wang Y 2015 *Angew. Chem. Int. Ed.* **54** 8369
[11] Zhang M X, Zhou Q, Zhang M R, Dai Y M, Song P and Jiang Y 2017 *J. Cluster Sci.* **28** 1191
[12] Jia X L, Li C Z, Li D L and Liu Y F 2018 *Spectrochim. Acta Part. A* **192** 168
[13] Han K L and Zhao G J 2011 *Hydrogen Bonding Transfer in the Excited State* (Chichester: John Wiley & Sons) p. 555
[14] Wu W R 2015 *J. Phys. Org. Chem.* **28** 596
[15] Yang D P, Zheng R, Wang Y S and Lv J 2016 *J. Phys. Org. Chem.* **29** 161
[16] Yang D P, Yang G, Zhao J F, Song N H, Zheng R and Wang Y S 2018 *J. Phys. Org. Chem.* **31** e3729
[17] Sen Gupta S K 2016 *J. Phys. Org. Chem.* **29** 251
[18] Yang D P, Yang G, Zhao J F, Zheng R, Wang Y S and Lv J 2017 *J. Phys. Org. Chem.* **30** e3684
[19] Padalkar V S and Seki S 2016 *Chem. Soc. Rev.* **45** 169
[20] Mei J, Leung N L C, Kwok R T K, Lam J W Y and Tang B Z 2015 *Chem. Rev.* **115** 11718
[21] Kumbhar H S and Shankarling G S 2015 *Dyes Pigm.* **122** 85
[22] Shreykar M R and Sekar N 2017 *J. Fluoresc.* **27** 1687
[23] Hong Y, Lam J W Y and Tang B Z 2009 *Chem. Commun.* 4332
[24] Dwivedi B K, Singh V D, Paitandi R P and Pandey D S 2018 *Chem. Phys. Chem.* **19** 2672
[25] Samanta S, Manna U and Das G 2017 *New J. Chem.* **41** 1064
[26] Samanta S, Goswami S, Hoque M N, Ramesh A and Das G 2014 *Chem. Commun.* **50** 11833
[27] Winnik F M 1993 *Chem. Rev.* **93** 587
[28] Sahoo D, Narayanaswami V, Kay C M and Ryan R O 2000 *Biochemistry* **39** 6594
[29] Chung L W, Sameera W M C, Ramozzi R, Page A J, Hatanaka M, Petrova G P, Harris T V, Li X, Ke Z F, Liu F Y, Li H B, Ding L N and Morokuma K 2015 *Chem. Rev.* **115** 5678
[30] Dapprich S, Komáromi I, Byun K S, Morokum K and Frisch M J 1999 *J. Mol. Struct. THEOCHEM* **461** 1
[31] Vreven T, Morokuma K, Farkas Ö Schlegel H B and Frisch M J 2003 *J. Comput. Chem.* **24** 760
[32] Yang D P, Yang Y G and Liu Y F 2014 *Spectrochim. Acta Part. A* **117** 379
[33] Song P, Li Y Z, Ma F C, Pullerits T and Sun M T 2013 *J. Phys. Chem. C* **117** 15879
[34] Yin H and Shi Y 2018 *Chin. Phys. B* **27** 058201
[35] Zhao G J and Han K L 2007 *J. Phys. Chem. A* **111** 2469
[36] Zhao G J and Han K L 2012 *Acc. Chem. Res.* **45** 404
[37] Yin H, Shi Y and Wang Y 2014 *Spectrochim. Acta Part. A* **129** 280
[38] Yin H, Li H, Xia G M, Ruan C Y, Shi Y, Wang H M, Jin M X and Ding D J 2016 *Sci. Rep.* **6** 19774
[39] Li C Z, Ma C, Li D L and Liu Y F 2016 *J. Lumin.* **172** 29
[40] Xu B B, Li Y Z, Song P, Ma F C and Sun M T 2017 *Sci. Rep.* **7** 45688
[41] Furche F and Ahlrichs R 2002 *J. Chem. Phys.* **117** 7433
[42] Li H, Ma L N, Yin H and Shi Y 2018 *Chin. Phys. B* **27** 098201
[43] Feller D 1996 *J. Comput. Chem.* **17** 1571
[44] Rappe A K, Casewit C J, Colwell K S, Goddard W A and Skiff W M 1992 *J. Am. Chem. Soc.* **114** 10024
[45] Rappe A K and Goddard W A 1991 *J. Phys. Chem.* **95** 3358
[46] Wang B, Wang X J, Wang W L and Liu F Y 2016 *J. Phys. Chem. C* **120** 21850
[47] Vreven T, Byun K S, Komáromi I, Dapprich S, Montgomery Jr J A, Morokuma K and Frisch M J 2006 *J. Chem. Theory Comput.* **2** 815
[48] Frisch M J *et al.* 2009 *Gaussian* 09 *Revision B.*01 (Gaussian, Inc., Wallingford)
[49] Lu T and Chen F W 2012 *J. Comput. Chem.* **33** 580
[50] Zhou P W and Han K L 2018 *Acc. Chem. Res.* **51** 1681